

Article

Identification of *miR-199-5p* and *miR-199-3p* Target Genes: Paxillin Facilitates Cancer Cell Aggressiveness in Head and Neck Squamous Cell Carcinoma

Nozomi Tanaka ^{1,†}, Chikashi Minemura ^{1,†}, Shunichi Asai ^{2,3}, Naoko Kikkawa ^{2,3}, Takashi Kinoshita ³, Sachi Oshima ¹, Ayaka Koma ¹, Atsushi Kasamatsu ¹, Toyoyuki Hanazawa ³, Katsuhiko Uzawa ¹ and Naohiko Seki ^{2,*}

- ¹ Department of Oral Science, Graduate School of Medicine, Chiba University, Chiba 260-8670, Japan; n.tanaka@chiba-u.jp (N.T.); minemura@chiba-u.jp (C.M.); Sachi.o8952@chiba-u.jp (S.O.); axna4812@chiba-u.jp (A.K.); kasamatsua@faculty.chiba-u.jp (A.K.); uzawak@faculty.chiba-u.jp (K.U.)
- ² Department of Functional Genomics, Graduate School of Medicine, Chiba University, Chiba 260-8670, Japan; cada5015@chiba-u.jp (S.A.); naoko-k@hospital.chiba-u.jp (N.K.)
- ³ Department of Otorhinolaryngology, Head and Neck Surgery, Graduate School of Medicine, Chiba University, Chiba 260-8670, Japan; t.kinoshita@chiba-u.jp (T.K.); thanazawa@faculty.chiba-u.jp (T.H.)
- * Correspondence: naoseki@faculty.chiba-u.jp; Tel.: +81-43-226-2971; Fax: +81-43-227-3442
- † These authors contributed equally to this work.



Citation: Tanaka, N.; Minemura, C.; Asai, S.; Kikkawa, N.; Kinoshita, T.; Oshima, S.; Koma, A.; Kasamatsu, A.; Hanazawa, T.; Uzawa, K.; et al. Identification of *miR-199-5p* and *miR-199-3p* Target Genes: Paxillin Facilitates Cancer Cell Aggressiveness in Head and Neck Squamous Cell Carcinoma. *Genes* **2021**, *12*, 1910. <https://doi.org/10.3390/genes12121910>

Academic Editors: Edoardo Alesse, Francesca Zazzeroni and Alessandra Tessitore

Received: 11 October 2021
Accepted: 24 November 2021
Published: 27 November 2021

Publisher's Note: MDPI stays neutral with regard to jurisdictional claims in published maps and institutional affiliations.



Copyright: © 2021 by the authors. Licensee MDPI, Basel, Switzerland. This article is an open access article distributed under the terms and conditions of the Creative Commons Attribution (CC BY) license (<https://creativecommons.org/licenses/by/4.0/>).

Abstract: Our previous study revealed that the *miR-199* family (*miR-199a-5p/-3p* and *miR-199b-5p/-3p*) acts as tumor-suppressive miRNAs in head and neck squamous cell carcinoma (HNSCC). Furthermore, recent studies have indicated that the passenger strands of miRNAs are involved in cancer pathogenesis. The aim of this study was to identify cancer-promoting genes commonly regulated by *miR-199-5p* and *miR-199-3p* in HNSCC cells. Our in silico analysis and luciferase reporter assay identified paxillin (*PXN*) as a direct target of both *miR-199-5p* and *miR-199-3p* in HNSCC cells. Analysis of the cancer genome atlas (TCGA) database showed that expression of *PXN* significantly predicted a worse prognosis (5-year overall survival rate; $p = 0.0283$). *PXN* expression was identified as an independent factor predicting patient survival according to multivariate Cox regression analyses ($p = 0.0452$). Overexpression of *PXN* was detected in HNSCC clinical specimens by immunostaining. Functional assays in HNSCC cells showed that knockdown of *PXN* expression attenuated cancer cell migration and invasion, suggesting that aberrant expression of *PXN* contributed to HNSCC cell aggressiveness. Our miRNA-based approach will provide new insights into the molecular pathogenesis of HNSCC.

Keywords: microRNA; HNSCC; *miR-199-5p*; *miR-199-3p*; paxillin; TCGA

1. Introduction

Global cancer statistics in 2018 stated that head and neck squamous cell carcinoma (HNSCC) was the eighth most common human malignancy worldwide [1]. Every year, there are approximately more than 800,000 new HNSCC cases diagnosed and 430,000 deaths from HNSCC [2]. HNSCC arises from the oral cavity, hypopharynx, nasopharynx, and larynx, and the most common subtype of HNSCC is oral squamous cell carcinoma (OSCC) [3]. There are regional differences in the frequency of HNSCC occurrence [4], and India and Sri Lanka are high-risk countries for HNSCC, accounting for more than 20% of all cancers [5].

Approximately 60% of patients with HNSCC are at an advanced stage at the time of diagnosis [6]. Aggressive progression of HNSCC is characterized by high rates of recurrence, distant metastasis, and drug resistance acquired by cancer cells during treatment [7]. To date, a number of treatment strategies, such as radiotherapy, chemoradiotherapy, molecular targeted agents and immune checkpoint inhibitors have been devised and implemented for HNSCC [8]. However, the treatment outcomes of HNSCC have not improved significantly

in recent decades, and the molecular mechanisms of malignant transformation of HNSCC are not completely understood.

A vast number of studies indicate that non-coding RNAs are involved in several biological processes, e.g., cell proliferation, apoptosis, development, epithelial-to-mesenchymal transition (EMT), and chromatin remodeling [9,10]. In human cancers, aberrant expression of non-coding RNAs closely contributes to malignant transformation, metastasis, and drug resistance [11]. However, the biological role and functions of non-coding RNAs are still mostly uncharacterized.

MicroRNA (miRNA) is small non-coding RNA that regulates the expression of RNA transcripts in normal and disease cells in a sequence-dependent manner [12]. A unique property of miRNAs is that a single miRNA can control a vast number of genes in a cell. In addition, the genes regulated by miRNAs vary from cell to cell. Therefore, aberrant expression of miRNAs disrupts intracellular transcriptional networks, which, in turn, causes human diseases, including cancers [13]. A growing body of evidence suggests that large non-coding RNAs act as miRNA sponges, reducing their regulatory effect on mRNAs [14]. It is likely that complex transcriptional regulatory networks involving long non-coding RNAs, miRNAs and protein-coding RNAs exist in cells. Elucidation of these complex RNA networks will lead to an understanding of the molecular pathogenesis of human cancers.

In the human genome, there are multiple miRNAs with the same mature miRNA sequence located at different positions on chromosomes; these constitute an miRNA family. Analysis of our miRNA signatures, determined by RNA sequencing, showed that the *miR-199* family is frequently downregulated in a wide range of cancer tissues [15]. The *miR-199* family is composed of three members, *miR-199a-1*, *miR-199a-2*, and *miR-199b*, located on human chromosomes 19p13.2, 1q24.3, and 9q34.11, respectively. In addition, two mature miRNAs (the guide strand and passenger strand) are derived from each pre-miRNA; thus, there are six miRNAs in the *miR-199* family. The guide strands of the *miR-199* family share the same seed sequence (CCAGUGU), and the passenger strands share the seed sequence (CAGUAGU). Analysis of our miRNA expression signatures of HNSCC and OSCC, determined by RNA sequencing, showed that the *miR-199* family is downregulated in cancer tissues [15–17]. Our previous study revealed that the *miR-199* family members are downregulated in HNSCC tissues, and ectopic expression of these miRNAs markedly attenuated cancer cell migration and invasive abilities [16]. It is important to identify the genes regulated by miRNAs in different cancer types. The aim of this study was to identify the *miR-199* gene targets closely involved in HNSCC oncogenesis. Our *in silico* analysis revealed that a total of 12 genes (*ABCA1*, *ADRBK2*, *ANKRD52*, *DEPDC1B*, *FXR1*, *ITGA3*, *KLF12*, *NLK*, *PCDH17*, *PDE7A*, *PXN*, and *SLC24A2*) are regulated by *miR-199-5p* and *miR-199-3p* in HNSCC cells. Among these targets, high expression of paxillin (*PXN*) and FMR1 autosomal homolog 1 (*FXR1*) significantly predicted the 5-year overall survival rate of patients with HNSCC. Furthermore, we demonstrated that aberrant expression of *PXN* facilitated cancer cell migration and invasion.

2. Materials and Methods

2.1. Identification of Putative Targets Controlled by *miR-199-5p* and *miR-199-3p* in HNSCC Cells

The sequences of members of the *miR-199* family were confirmed using miRbase ver. 22.1 (<https://www.mirbase.org>, accessed on 10 April 2020) [18]. A flowchart of the procedure used to identify common target genes of *miR-199-5p* and *miR-199-3p* in this study is shown in Figure 1. We selected putative target genes that had both *miR-199-5p* and *miR-199-3p*-binding sites using TargetScanHuman ver. 7.2 (http://www.targetscan.org/vert_72/; data downloaded on 10 July 2020) [19]. The candidate genes were narrowed down by analyzing HNSCC clinical information obtained from The Cancer Genome Atlas (TCGA-HNSC).

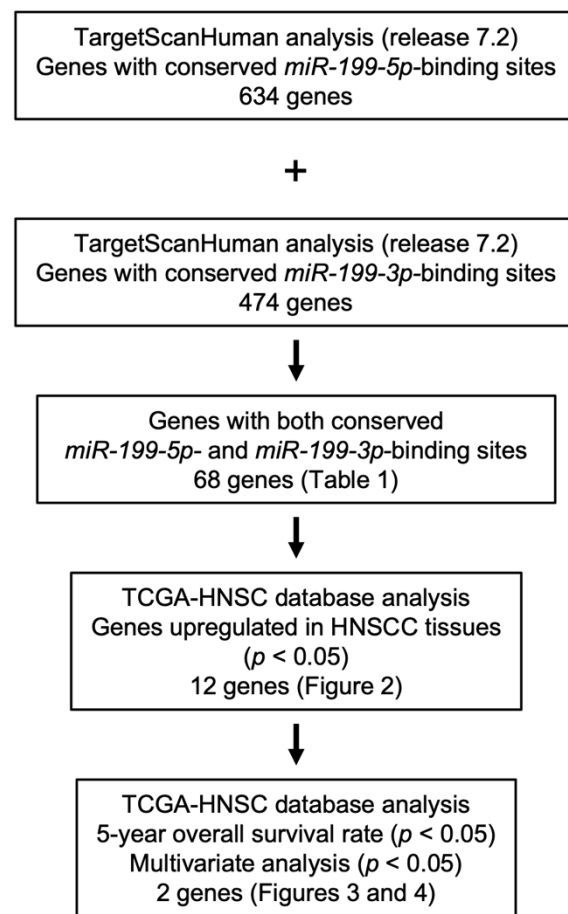


Figure 1. Flowchart of the strategy used to identify candidate *miR-199-5p* and *miR-199-3p* target genes in HNSCC cells.

For the Kaplan–Meier survival analysis and multivariate Cox regression analysis, we downloaded TCGA-HNSC clinical data (TCGA, Firehose Legacy) from cBioportal (<https://www.cbioportal.org>, accessed on 10 April 2020). Expression data for each gene were collected from OncoLnc (<http://www.oncolnc.org>; accessed on 20 April 2021) [20]. Patients from TCGA-HNSC were divided into low and high *FXR1/PXN* expression groups based on the median gene expression level, and the log-rank test was performed to compare the 5-year overall survival rate between the groups. In addition, Cox proportional hazards regression was conducted, using gene expression levels, tumor stage, pathological grade, and age as covariates.

We used JMP Pro 15 (SAS Institute Inc., Cary, NC, USA) to perform the log-rank test and Cox proportional hazards regression.

2.2. Gene set Enrichment Analysis (GSEA)

To analyze the molecular pathways related to *FXR1* and *PXN* (regulated by *miR-199a-5p* and *3p*), we performed GSEA. Using TCGA-HNSC data, we divided HNSCC patients into high and low expression groups according to the Z-score of the *FXR1* or *PXN* expression level. A ranked list of genes was generated by log₂ ratio comparing the expression levels of each gene between the two groups. The genes upregulated in the high expression groups were ranked higher. The obtained gene lists were uploaded into GSEA software [21,22]. We used KEGG subset of canonical pathways in The Molecular Signatures Database [21,23].

2.3. HNSCC Cell Lines

The HNSCC cell lines (SAS and Sa3) used in this study were obtained from the RIKEN BioResource Center (Tsukuba, Ibaraki, Japan). The characteristics of the cell lines are shown in Supplementary Table S1.

2.4. Transfection of Mature miRNAs and Small-Interfering RNAs (siRNAs) into HNSCC Cells

The miRNA precursors, negative control miRNA, and siRNAs were obtained from Invitrogen/Thermo Fisher Scientific (Waltham, MA, USA). The procedures used for transient transfection of miRNAs, siRNAs, and plasmid vectors have been described in our previous studies [16,17,24]. The reagents used are listed in Supplementary Table S2. All miRNAs and siRNA were transfected into HNSCC cell lines at 10 nM using RNAiMAX.

2.5. RNA Extraction and Quantitative Reverse-Transcription PCR (qRT-PCR)

RNA extraction from HNSCC cell lines and qRT-PCR were performed as described in our previous studies [16,17,24]. Briefly, total RNA was harvested using Trizol reagent and the PureLink™ RNA Mini Kit (Invitrogen/Thermo Fisher Scientific, Waltham, MA, USA). Reverse transcription was performed using the High-Capacity cDNA Reverse Transcription Kit (Applied Biosystems, Waltham, MA, USA). qRT-PCR was performed using the StepOnePlus™ Real-Time PCR System (Applied Biosystems). *GAPDH* was used as the internal control.

2.6. Immunohistochemistry

The immunohistochemistry procedures have been described in our previous studies [16,17,24]. Briefly, paraffin sections of tumors were obtained from HNSCC patients who underwent surgical treatment at Chiba University hospital. The clinical features of the HNSCC patients are summarized in Table S3. Our study was approved by the Ethics Committee of Chiba University (approval number: 28–65, 10 February 2015). Specimens were incubated with primary anti-PXN antibody overnight at 4 °C, after which they were incubated with DAKO Env+ secondary antibody for 30 min, washed, and counterstained with hematoxylin.

2.7. Western Blotting

The Western blotting procedures have been described in our previous studies [16,17,24]. Briefly, cell lysates were loaded onto 4–15% polyacrylamide gels at 18 µg/well. The proteins were transferred to polyvinylidene fluoride membranes and incubated with the primary antibody overnight at 4 °C and with the secondary antibody for 1 h. GAPDH was used as internal control.

2.8. Dual Luciferase Reporter Assays

A PXN DNA sequence with or without the miRNA-binding sequence of interest in its 3' untranslated region (UTR) was inserted into the psiCHECK-2 vector (C8021; Promega, Madison, WI, USA). The plasmid vectors were then transfected into cells using Lipofectamine 2000 (Invitrogen, Waltham, MA, USA) at a final concentration of 50 ng/well. After 48 h of transfection, dual luciferase reporter assays were performed using the Dual Luciferase Reporter Assay System (Promega, Madison, WI, USA). Normalized data are expressed as the Renilla/Firefly luciferase activity ratio.

2.9. Cell Proliferation, Migration, and Invasion Assays in HNSCC Cells

The XTT assay to assess cell proliferation, and the Matrigel chamber assay to assess invasion, were performed in HNSCC cells as described previously [16,17,24]. In the wound healing assay, to assess migration a wound was created using a micropipette tip in the middle of each plate of cells transfected with siRNAs for 48 h. We incubated the plates at 37 °C and captured live cell migration after 6 and 12 h.

2.10. Statistical Analysis

Statistical analyses were performed using JMP Pro 15 (SAS Institute Inc., Cary, NC, USA). Differences between two groups were evaluated by Welch's *t*-test. Dunnett's test was used for multiple group comparisons. A *p*-value < 0.05 was considered statistically significant. The bar graphs present means and standard errors.

3. Results

3.1. Identification of miR-199-5p and miR-199-3p Coordinately Regulated Genes in HNSCC Cells

Chromosomal locations and mature sequences of the miR-199 family are shown in Supplementary Figure S1. In humans, the miR-199 family is composed of three members, miR-199a-1, miR-199a-2, and miR-199b, located on human chromosomes 19p13.2, 1q24.3, and 9q34.11, respectively. The guide strands of the miR-199 family share the same seed sequence (CCAGUGU); the passenger strands share same sequence (CAGUAGU).

TCGA database analysis showed the downregulation of all members of the miR-199 family in HNSCC clinical tissues (Supplementary Figure S2). At first, we confirmed tumor-suppressive functions of miR-199-5p and miR-199-3p in HNSCC cells by ectopic expression assays. Expression of miR-199-5p and miR-199-3p did not affect cell proliferation in SAS and Sa3 cells (Supplementary Figure S3A). Cell invasion and migration features were markedly suppressed by miR-199-5p and miR-199-3p expression in SAS and Sa3 cells (Supplementary Figure S3B,C). Typical images of cells from the invasion and migration assays are shown in Supplementary Figures S4 and S5. These data clearly show that both miR-199-5p and miR-199-3p acted as tumor-suppressive miRNAs in HNSCC cells.

The flowchart in Figure 1 shows the procedure we used to identify target genes of miR-199-5p and miR-199-3p. First, we searched for putative miR-199-5p- and miR-199-3p-binding genes in the TargetScan database (release 7.2). We found 634 and 474 transcripts that contained conserved miR-199-5p- and miR-199-3p-binding sites in their 3'UTRs, respectively. Of these transcripts, 68 transcripts possessed putative binding sites for both miR-199-5p and miR-199-3p (Table 1).

3.2. Expression and Clinical Significance of the Putative Target Genes in Patients with HNSCC according to TCGA Analysis

The expression levels of the putative targets (68 genes) of miR-199-5p and miR-199-3p were evaluated using the TCGA database (TCGA-HNSC). Among these genes, the expression levels of 12 genes (*ABCA1*, *ADRBK2*, *ANKRD52*, *DEPDC1B*, *FXR1*, *ITGA3*, *KLF12*, *NLK*, *PCDH17*, *PDE7A*, *PXN*, and *SLC24A2*) were significantly upregulated in HNSCC tissues (*n* = 518) compared with normal tissues (*n* = 44) (Figure 2). Among these 12 genes, *DEPDC1B* had a negative correlation with the miR-199 family in cancer tissues according to Spearman's rank test (Supplementary Figure S6).

Table 1. miR-199-5p/3p common target genes.

Entrez Gene ID	Gene Symbol	Gene Name	miR-199-5p Total Conserved Sites	miR-199-3p Total Conserved Sites
19	<i>ABCA1</i>	ATP-binding cassette, sub-family A (ABC1), member 1	1	1
340485	<i>ACER2</i>	alkaline ceramidase 2	1	1
92	<i>ACVR2A</i>	activin A receptor, type IIA	1	2
93	<i>ACVR2B</i>	activin A receptor, type IIB	3	1
57188	<i>ADAMTSL3</i>	ADAMTS-like 3	1	3
120	<i>ADD3</i>	adducin 3 (γ)	1	1
157	<i>ADRBK2</i>	adrenergic, beta, receptor kinase 2	1	1
81573	<i>ANKRD13C</i>	ankyrin repeat domain 13C	1	1
283373	<i>ANKRD52</i>	ankyrin repeat domain 52	1	1
57569	<i>ARHGAP20</i>	Rho GTPase activating protein 20	1	1
23365	<i>ARHGEF12</i>	Rho guanine nucleotide exchange factor (GEF) 12	1	1
222255	<i>ATXN7L1</i>	ataxin 7-like 1	1	1
27443	<i>CECR2</i>	cat eye syndrome chromosome region, candidate 2	2	1
10659	<i>CELF2</i>	CUGBP, Elav-like family member 2	1	2
387119	<i>CEP85L</i>	centrosomal protein 85kDa-like	1	1

Table 1. Cont.

Entrez Gene ID	Gene Symbol	Gene Name	miR-199-5p Total Conserved Sites	miR-199-3p Total Conserved Sites
153222	CREBRF	CREB3 regulatory factor	1	1
51232	CRIM1	cysteine rich transmembrane BMP regulator 1 (chordin-like)	1	1
1496	CTNNA2	catenin (cadherin-associated protein), $\alpha 2$	1	1
84301	DDI2	DNA-damage inducible 1 homolog 2 (<i>S. cerevisiae</i>)	1	1
55789	DEPDC1B	DEP domain containing 1B	1	1
2066	ERBB4	v-erb-b2 avian erythroblastic leukemia viral oncogene homolog 4	1	2
55137	FIGN	fidgetin	1	1
23767	FLRT3	fibronectin leucine rich transmembrane protein 3	1	1
10690	FUT9	fucosyltransferase 9 (α (1,3) fucosyltransferase)	1	1
8087	FXR1	fragile X mental retardation, autosomal homolog 1	2	1
2651	GCNT2	glucosaminyl (N-acetyl) transferase 2, I-branching enzyme (I blood group)	1	1
54891	INO80D	INO80 complex subunit D	1	1
3675	ITGA3	integrin, $\alpha 3$ (antigen CD49C, $\alpha 3$ subunit of VLA-3 receptor)	1	1
8516	ITGA8	integrin, $\alpha 8$	1	1
11278	KLF12	Kruppel-like factor 12	1	1
26249	KLHL3	kelch-like family member 3	1	3
84458	LCOR	ligand dependent nuclear receptor corepressor	2	2
10960	LMAN2	lectin, mannose-binding 2	1	1
84061	MAGT1	magnesium transporter 1	1	1
4217	MAP3K5	mitogen-activated protein kinase 5	1	1
5599	MAPK8	mitogen-activated protein kinase 8	1	1
90411	MCFD2	multiple coagulation factor deficiency 2	1	1
54842	MFSD6	major facilitator superfamily domain containing 6	1	1
51701	NLK	nemo-like kinase	3	1
57532	NUFIP2	nuclear fragile X mental retardation protein interacting protein 2	1	1
10298	PAK4	p21 protein (Cdc42/Rac)-activated kinase 4	1	2
27253	PCDH17	protocadherin 17	1	1
5150	PDE7A	phosphodiesterase 7A	1	1
57475	PLEKHH1	pleckstrin homology domain containing, family H (with MyTH4 domain) member 1	1	1
5495	PPM1B	protein phosphatase, Mg^{2+}/Mn^{2+} dependent, 1B	1	1
55607	PPP1R9A	protein phosphatase 1, regulatory subunit 9A	1	1
63976	PRDM16	PR domain containing 16	1	1
5813	PURA	purine-rich element binding protein A	1	1
5829	PXN	paxillin	1	1
5925	RB1	retinoblastoma 1	1	1
54502	RBM47	RNA binding motif protein 47	1	1
5991	RFX3	regulatory factor X, 3 (influences HLA class II expression)	1	1
6096	RORB	RAR-related orphan receptor B	1	2
9644	SH3PXD2A	SH3 and PX domains 2A	1	1
25769	SLC24A2	solute carrier family 24 (sodium/potassium/calcium exchanger), member 2	1	1
8303	SNN	stannin	1	1
6667	SP1	Sp1 transcription factor	1	1
257397	TAB3	TGF- β activated kinase 1/MAP3K7 binding protein 3	1	1
57551	TAOK1	TAO kinase 1	1	2
10099	TSPAN3	tetraspanin 3	1	1
57695	USP37	ubiquitin specific peptidase 37	1	1
23063	WAPAL	wings apart-like homolog (<i>Drosophila</i>)	1	2
10472	ZBTB18	zinc finger and BTB domain containing 18	1	2
26137	ZBTB20	zinc finger and BTB domain containing 20	2	2
6935	ZEB1	zinc finger E-box binding homeobox 1	1	1
80139	ZNF703	zinc finger protein 703	1	1
374655	ZNF710	zinc finger protein 710	1	1
283337	ZNF740	zinc finger protein 740	1	1

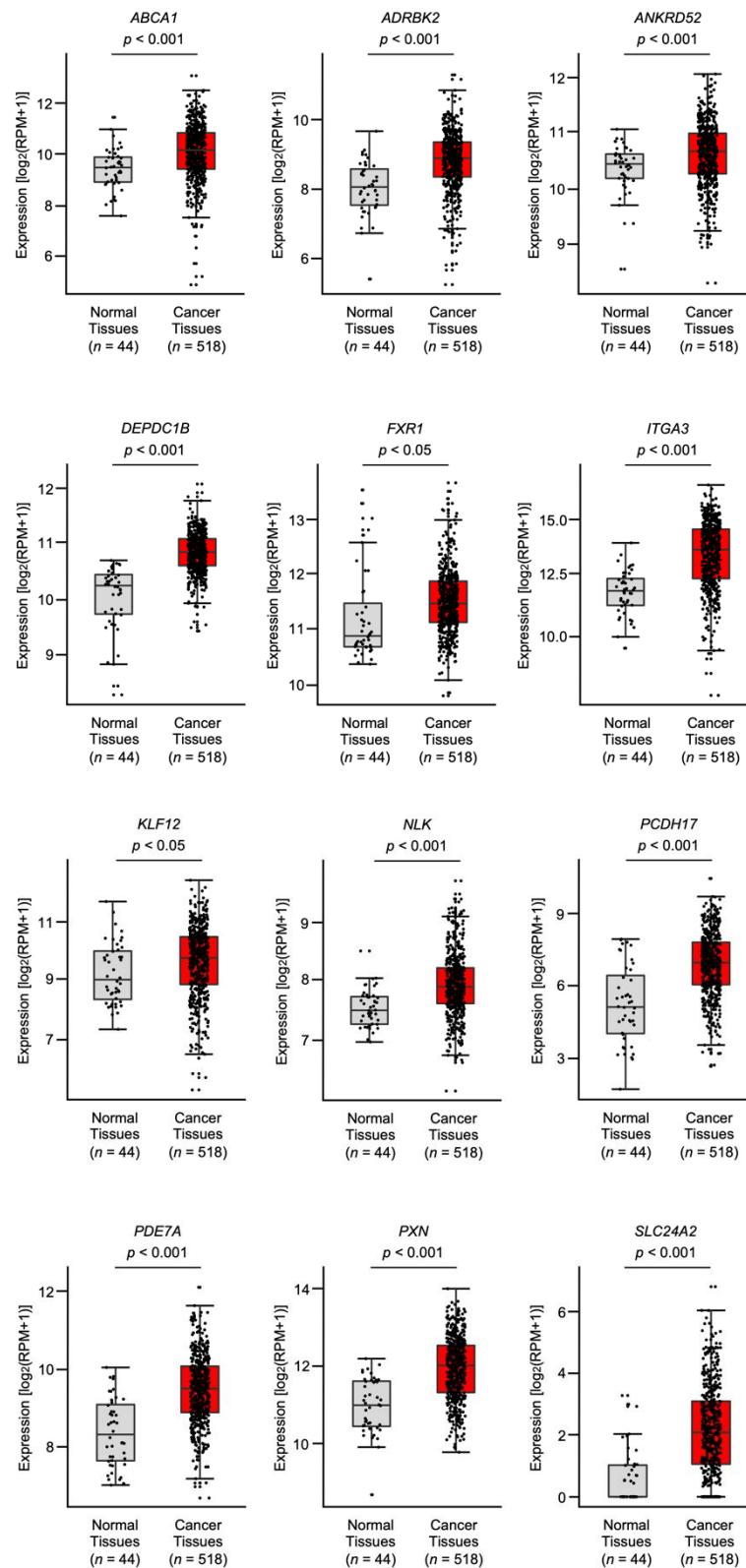


Figure 2. HNSCC tissue expression of 12 target genes with *miR-199-5p*- and *miR-199-3p*-binding sites in their 3'UTRs using TCGA-HNSC data. The expression levels of 12 genes (*ABCA1*, *ADRBK2*, *ANKRD52*, *DEPDC1B*, *FXR1*, *ITGA3*, *KLF12*, *NLK*, *PCDH17*, *PDE7A*, *PXN*, and *SLC24A2*) were analyzed using TCGA-HNSC database. A total of 518 HNSCC tissues and 44 normal epithelial tissues were evaluated.

To determine clinical relevance, the 5-year overall survival rates of HNSCC patients according to the expression levels of these 12 genes were determined using TCGA-HNSC data. Patients with high expression of either *FXR1* ($p = 0.0003$) or *PXN* ($p = 0.0283$) had a significantly worse prognosis compared with those with low expression (Figure 3). Moreover, multivariate Cox regression analysis revealed that the expression levels of *FXR1* ($p = 0.0017$) and *PXN* ($p = 0.0452$) were independent prognostic factors in patients with HNSCC (Figure 3).

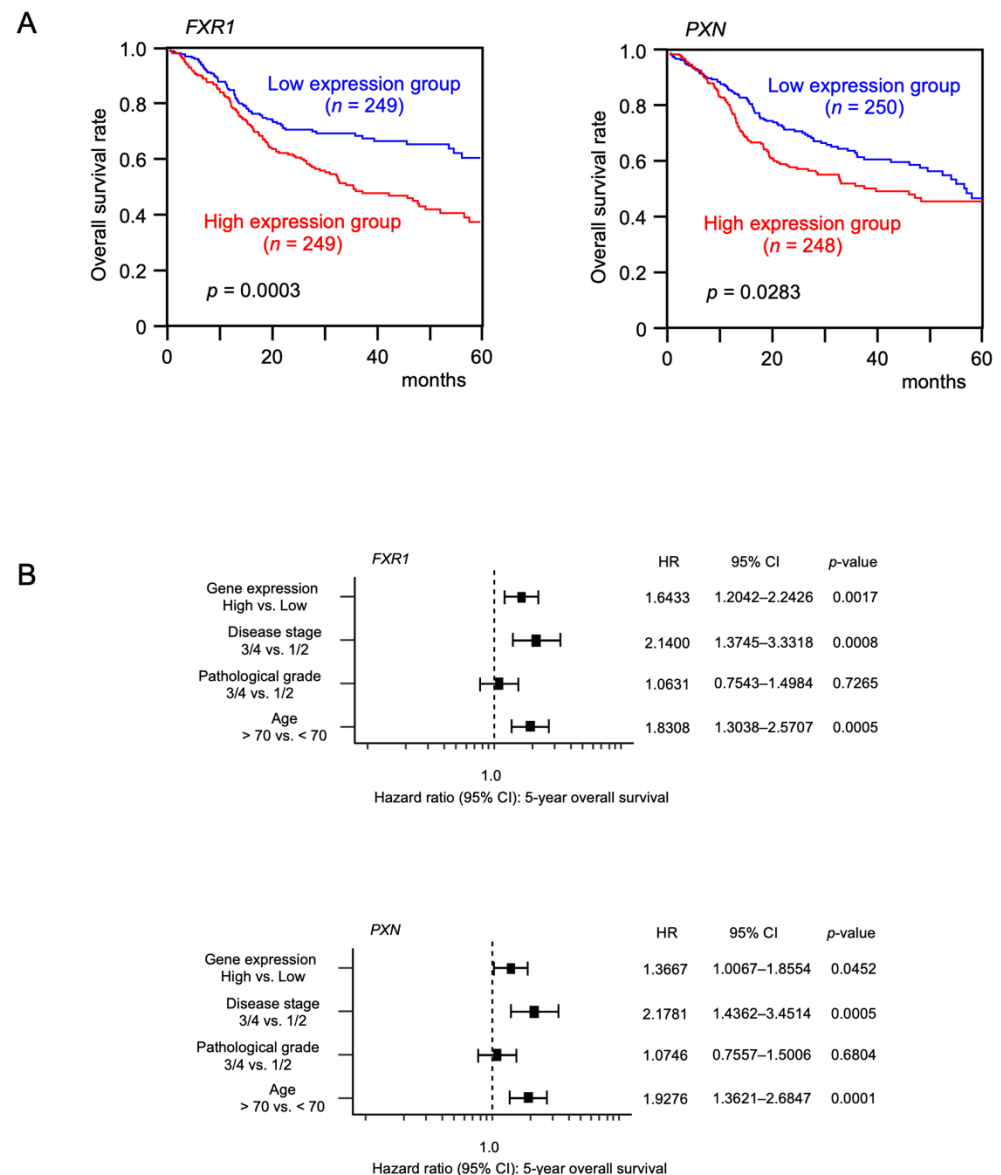


Figure 3. Clinical significance of *FXR1* and *PXN* using TCGA-HNSC data. **(A)** Kaplan–Meier survival analyses of HNSC patients using data from TCGA database. Patients were divided into high and low expression groups according to the median *FXR1* and *PXN* expression levels. The red and blue lines indicate the high and low expression groups, respectively. **(B)** Forest plot showing the multivariate analysis results for two genes (*FXR1* and *PXN*), which were identified as independent prognostic factors for overall survival after adjustment for patient age, disease stage, and pathological grade.

3.3. *FXR1*- and *PXN*-Mediated Pathways in HNSCC Cells

We investigated the genes differentially expressed between the high and low *FXR1* or *PXN* expression groups in the HNSCC cohort from TCGA using GSEA. A total of four and fourteen gene sets were significantly enriched (FDR q -value < 0.05) in the high *FXR1* and

PXN expression groups, respectively (Table 2B). The most enriched gene set in the high *FXR1* expression group was the cardiac muscle contraction KEGG pathway, whereas that in the high *PXN* expression group was the focal adhesion KEGG pathway. Although both *FXR1* and *PXN* were involved in the prognosis of HNSCC, based on our *in silico* analyses, the results of GSEA analysis suggested that *FXR1* was mainly involved in the pathogenesis of myocardial function. HNSCC is characterized by high rates of local recurrence and distant metastasis. Therefore, we focused on the roles of *PXN* in the KEGG pathways of focal adhesion and ECM receptor interaction, which are closely associated with local recurrence and distant metastasis, by performing functional analyses.

Table 2. Gene set enrichment analysis.

A. Significantly Enriched Gene Sets in the High <i>FXR1</i> Expression Group		
Name	Normalized Enrichment Score	FDR <i>q</i> -Value
KEGG_Cardiac muscle contraction	2.009	0.001
KEGG_Dilated cardiomyopathy	1.968	0.001
KEGG_Hypertrophic cardiomyopathy HCM	1.929	0.003
KEGG_Maturity onset diabetes of the young	1.918	0.002
B. Significantly enriched gene sets in the high <i>PXN</i> expression group		
Name	normalized enrichment score	FDR <i>q</i> -value
KEGG_Focal adhesion	2.458	$q < 0.001$
KEGG_ECM receptor interaction	2.316	$q < 0.001$
KEGG_Cytosolic DNA sensing pathway	2.117	0.001
KEGG_Proteasome	2.029	0.003
KEGG_Hypertrophic cardiomyopathy HCM	1.995	0.005
KEGG_NOD-like receptor signaling pathway	1.896	0.009
KEGG_Viral myocarditis	1.894	0.008
KEGG_Dilated Cardiomyopathy	1.804	0.014
KEGG_Bladder cancer	1.784	0.016
KEGG_Cytokine cytokine receptor interaction	1.776	0.016
KEGG_JAK/STAT signaling pathway	1.712	0.026
KEGG_RIG-I-like receptor signaling pathway	1.673	0.033
KEGG_Small cell lung cancer	1.644	0.038
KEGG_Arrhythmogenic right ventricular cardiomyopathy ARVC	1.639	0.037

3.4. Expression of *PXN* in HNSCC Clinical Specimens

Expression of *PXN* protein was investigated by immunostaining in HNSCC clinical specimens. Aberrant expression of *PXN* was detected in HNSCC lesions (Figure 4). In contrast, there was almost no *PXN* expression in the normal epithelium (Figure 4).

3.5. Regulation of *PXN* Expression by *miR-199-5p* and *miR-199-3p* in HNSCC Cells

Both the mRNA and protein levels of *PXN* were reduced after *miR-199-5p* and *miR-199-3p* transfection in SAS and Sa3 cells (Figure 5A,B). Full-size Western blots are shown in Supplementary Figure S7.

To investigate whether *miR-199-5p* and *miR-199-3p* bind directly to *PXN* in HNSCC cells, we conducted a dual-luciferase reporter assay. Luciferase activity was significantly reduced following cotransfection with *miR-199-5p* and a vector containing the *miR-199-5p*-binding site in the 3'UTR of *PXN*. On the other hand, cotransfection with a vector containing the *PXN* 3'UTR in which the *miR-199-5p*-binding site was deleted resulted in no change in luciferase activity (Figure 5C).

Similar to *miR-199-5p*, luciferase activity was significantly reduced following cotransfection with *miR-199-3p* and a vector containing the *miR-199-3p*-binding site in the 3'UTR of *PXN*, but not with a vector lacking the *miR-199-3p*-binding site in the *PXN* 3'UTR (Figure 5D).

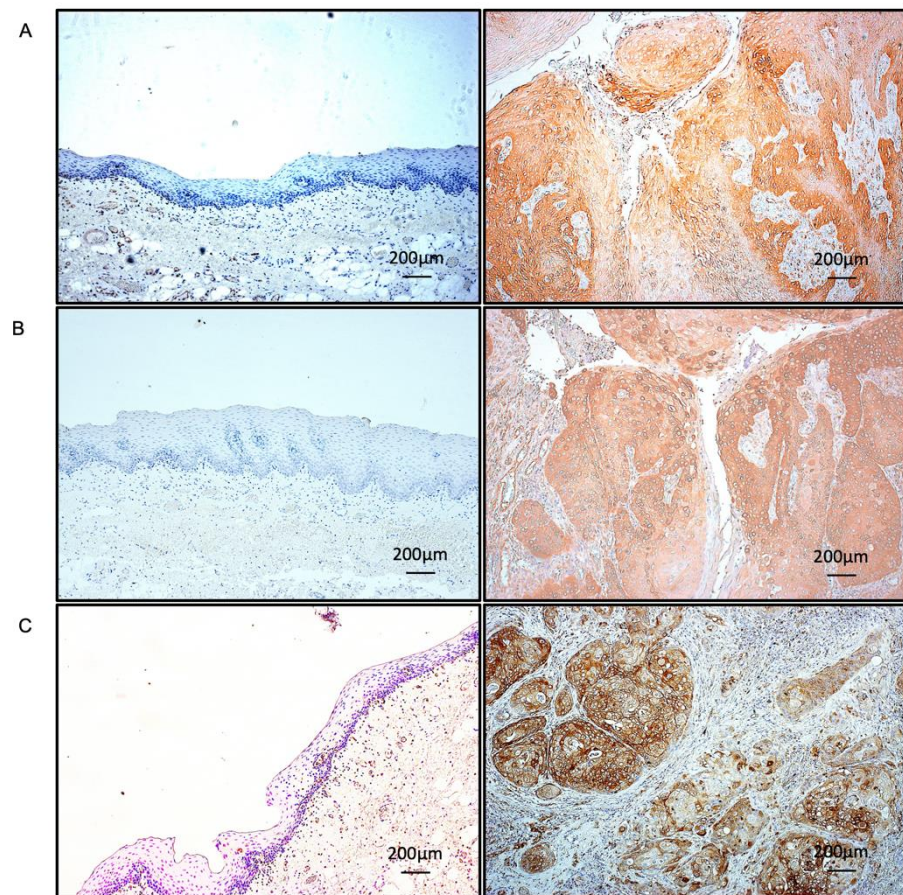
These findings suggest that *miR-199-5p* and *miR-199-3p* bind directly to the 3'UTR of *PXN* and regulate the expression of *PXN* in HNSCC cells.

3.6. Effects of *PXN* Knockdown on the Proliferation, Invasion and Migration of HNSCC Cells

To assess the tumor-promoting effect of *PXN* in HNSCC cells, we performed knock-down assays using siRNAs. First, the inhibitory effects of three different siRNAs targeting *PXN* (si*PXN*-1, si*PXN*-2 and si*PXN*-3) on *PXN* expression were examined. The *PXN* mRNA and protein levels were effectively suppressed after transfection of each siRNA into SAS and Sa3 cells (Supplementary Figure S8A,B). For the subsequent functional assays in HNSCC cells, we used si*PXN*-1 and si*PXN*-3.

Knockdown of *PXN* had a slight inhibitory effect on cell proliferation in SAS and Sa3 cells (Figure 6A), and cell invasion and migration were significantly inhibited after si*PXN*-1 and si*PXN*-3 transfection in SAS and Sa3 cells (Figure 6B,C). Experimental photographs of typical results from the invasion and wound healing assays are shown in Supplementary Figures S9 and S10.

These findings indicate that overexpression of *PXN* is involved in promoting cancer cell migration and invasion.



(× 200)

Figure 4. Overexpression of *PXN* in HNSCC clinical specimens. (A–C) Immunohistochemical staining of *PXN* in HNSCC clinical specimens. *PXN* expression was high in the nuclei and/or cytoplasm of cancer cells (right panels) but weak in normal mucosa (left panels).

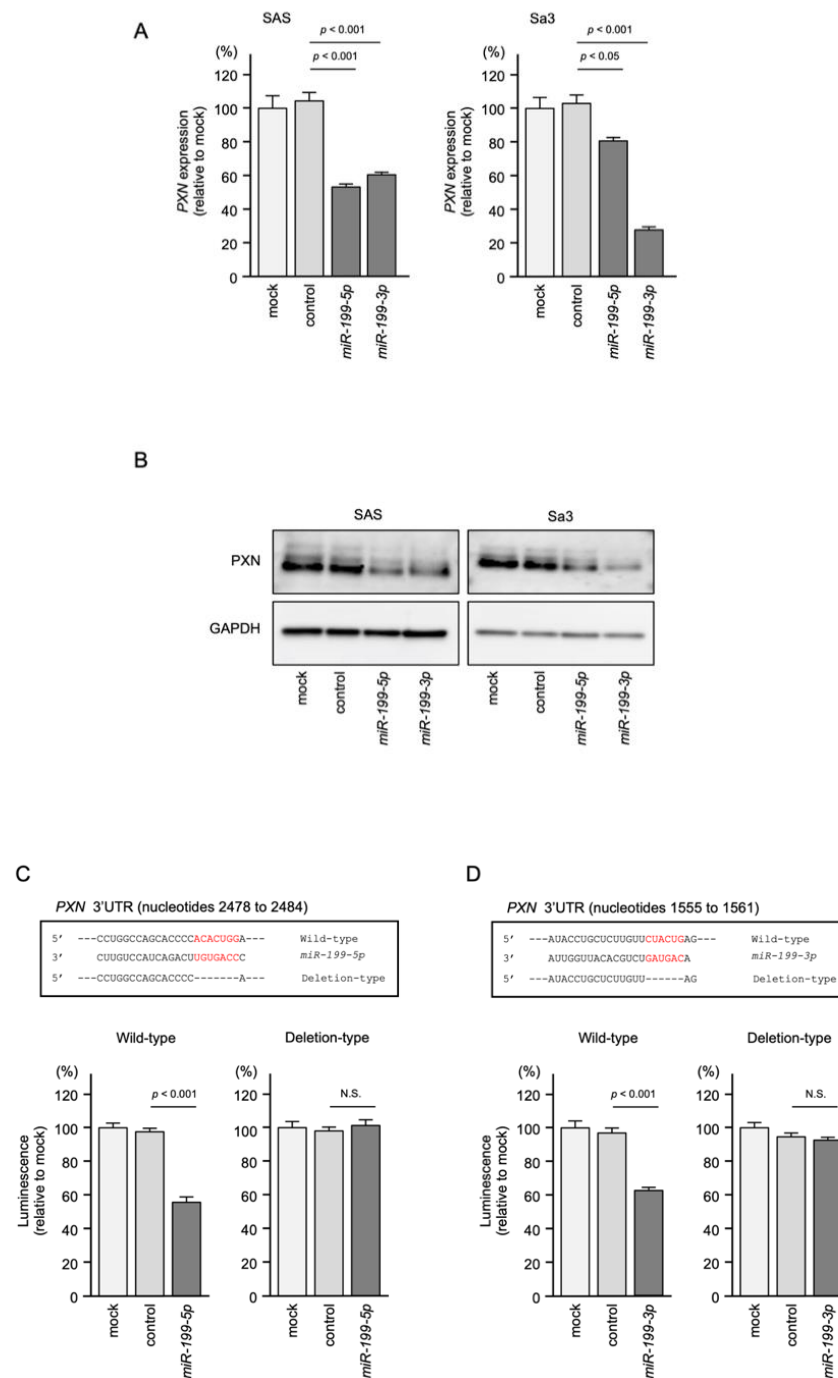


Figure 5. Direct regulation of *PXN* expression by both *miR-199-5p* and *miR-199-3p* in HNSCC cells. (A) qRT-PCR showing significantly reduced expression of *PXN* mRNA at 72 h after *miR-199-5p* or *miR-199-3p* transfection in SAS and Sa3 cells. Expression of *GAPDH* was used as an internal control. (B) Western blot showing reduced expression of *PXN* protein at 72 h after *miR-199-5p* or *miR-199-3p* transfection in SAS and Sa3 cells. Expression of *GAPDH* was used as an internal control. (C) TargetScan database analysis predicting a single putative *miR-199-5p*-binding site in the 3'-UTR of *PXN* (upper panel). Dual luciferase reporter assays showed reduced luminescence activity after cotransfection of the wild-type vector and *miR-199-5p* in SAS cells (lower panel). Normalized data are expressed as the Renilla/Firefly luciferase activity ratio (N.S., not significant). (D) TargetScan database analysis predicting a single putative *miR-199-3p*-binding site in the 3'-UTR of *PXN* (upper panel). Dual luciferase reporter assays showed reduced luminescence activity after cotransfection of the wild-type vector and *miR-199-3p* in SAS cells (lower panel).

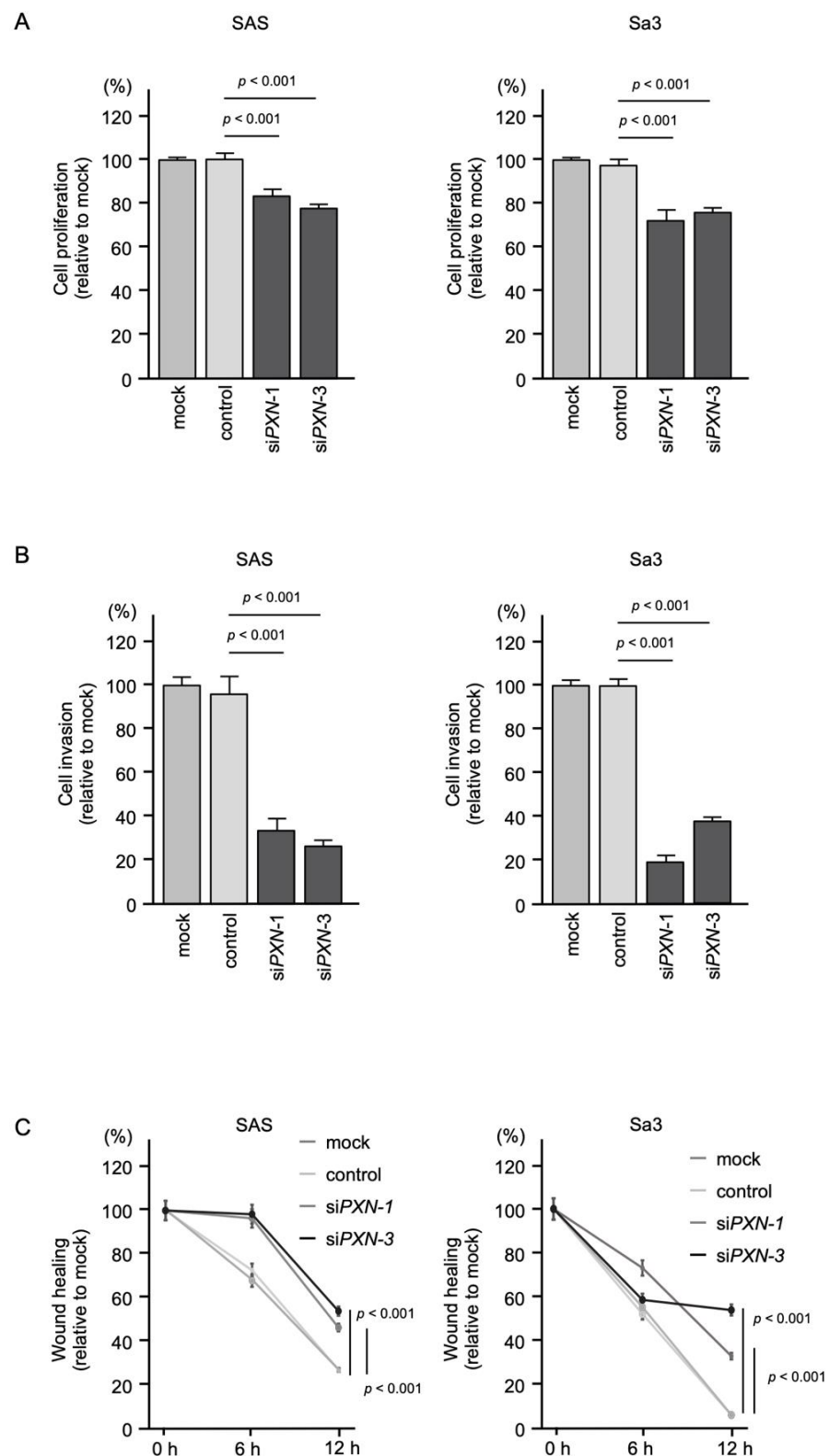


Figure 6. Functional assays of cell proliferation, invasion and migration following transient transfection of siRNAs targeting *PXN* in HNSCC cell lines (SAS and Sa3 cells). **(A)** Cell proliferation assessed by XTT assay at 72 h after siRNA transfection. **(B)** Cell invasion assessed by Matrigel invasion assays at 48 h after seeding siRNA-transfected cells into chambers. **(C)** Cell migration assessed by wound healing assay at 0, 6, and 12 h after cell scratch formation.

4. Discussion

Currently available RNA sequencing technologies are suitable for creating miRNA expression signatures in various types of human cancers [25]. Analysis of our miRNA expression signatures in cancers revealed that some passenger strands of miRNAs derived from pre-miRNAs (e.g., *miR-31-3p*, *miR-145-3p*, *miR-99a-3p*, and *miR-139-3p*) are dysregulated in HNSCC tissues. Moreover, our functional assays showed that these passenger strands contribute to HNSCC oncogenesis, and that several of their target genes are closely associated with HNSCC pathogenesis [17,24,26,27].

Recently, a large number of TCGA cohort studies showed that certain miRNAs (e.g., both the 5p and 3p strands of *miR-29*, *miR-30a*, *miR-143*, *miR-145*, and *miR-139*) coordinately regulate oncogenic pathways in cancer cells [28]. In opposition to the traditional concept of miRNA biogenesis, the involvement of miRNA passenger strands in cancer pathogenesis is a newly proposed concept. Therefore, searching for target genes of miRNA passenger strands, as well as guide strands, is an important issue in cancer research.

Previous studies have reported that *miR-199* family members are closely implicated in a variety of cancers as either tumor-suppressors or oncogenes [29]. Expression of *miR-199a-5p* was significantly reduced in OSCC tissues, and its overexpression blocked the EMT cascade by targeting *SOX4* [30]. Another study showed that transient transfection of *miR-199a-5p* suppressed the malignant phenotypes of OSCC cells, for example, blocking cell proliferation and inducing G0/G1 arrest and apoptosis. This study indicated that IKK β , a pivotal activator of NF- κ B, is a direct target of *miR-199a-5p* [31].

Our next focus was to identify oncogenic targets regulated by both *miR-199-5p* and *miR-199-3p* in HNSCC cells. Our in silico analysis revealed that *FXR1* and *PXN* are candidate targets of *miR-199-5p* and *miR-199-3p* in HNSCC cells. Importantly, expression of *FXR1* and *PXN* was closely associated with the molecular pathogenesis of HNSCC.

Overexpression of *FXR1*, an RNA-binding protein, has been reported in a wide range of cancers, including HNSCC and oral cancer [32–35]. Previous studies showed that overexpressed *FXR1* promoted cancer cell aggressiveness by binding to and disrupting p21 mRNA [36]. Interestingly, in oral cancer cells, *FXR1* stabilized *miR-301a-3p*, and these events reduced expression of p21 [37]. How aberrantly expressed *FXR1* is involved in miRNA networks in HNSCC cells is an important question.

PXN is an intercellular adaptor protein that interacts with multiple proteins involved in cell adhesion [38]. Notably, *PXN* can connect integrins to focal adhesion kinase (FAK) and is a pivotal player in the assembly and disassembly of focal adhesions [39]. FAK is an important molecule that acts as a relay station for signals mediated by integrins or receptor tyrosine kinase, such as cytoskeletal changes, lamellipodia formation, cell proliferation and motility [40]. Aberrant activation of FAK-mediated signaling enhances cell proliferation, invasion, and metastasis [41]. Previous studies showed that aberrant expression of *PXN* was detected in a wide range of cancers, and its overexpression was usually correlated with worse prognosis of the patients [42]. However, in some types of cancers, downregulation of *PXN* was reported, e.g., breast cancer, colorectal cancer, leukemia, and low-grade glioma [43]. Here, we clearly showed that overexpression of *PXN* closely contributes to malignant transformation of HNSCC cells and a worse patient prognosis. It is an interesting finding that the expression of *PXN* differs depending on the type of cancer. Analysis of the epigenetic modification that regulates *PXN* expression is required for each cancer type. In HNSCC cells, analysis of *PXN* and *PXN*-mediated downstream signals will aid the search for therapeutic target molecules for this disease.

Recent reports have shown that several dysregulated non-coding RNAs (long non-coding RNAs [lncRNAs] and miRNAs) are involved in aberrant expression of *PXN* in cancer cells [44–46]. Overexpressed lncRNAs were found to adsorb tumor-suppressor miRNAs and suppress their antitumor effects in cancer cells [47–50]. In gastric cancer, the lncRNA *XIST*, when overexpressed, adsorbed *miR-132* and caused upregulation of *PXN* in cancer cells. This study found that *XIST* acts as an oncogenic lncRNA in gastric cancer [51]. In triple-negative breast cancer, the lncRNA *DLX6* antisense RNA 1 was upregulated in

cancer tissues, and its expression promoted cell proliferation, EMT, and cisplatin resistance by regulating the *miR-199b-5p/PXN* axis [52]. These data support our current results. It is expected that many lncRNAs are involved in suppression of *miR-199* family expression in HNSCC cells.

A previous study showed that expression of *miR-218* was reduced by human papillomavirus-16 (HPV-16) in cervical cancer [53]. In HPV-16-infected OSCC cells, downregulation of *miR-218* and upregulation of *PXN* were detected, and these events contributed to colony formation and invasion of OSCC cells [54]. Moreover, low expression of *miR-218*, or high expression of *PXN*, was closely associated with overall survival and relapse-free survival [55]. Our previous studies demonstrated that *miR-218* acts as a tumor-suppressive miRNA in HNSCC by markedly suppressing cancer cell migration and invasive abilities [56]. Suppression of *miR-218* expression might be linked to aberrant expression of *PXN* in HNSCC cells.

Many non-coding RNA molecules are involved in the regulation of *PXN* expression, and the complexity of the molecular mechanisms of cancer cells has been clarified. To clarify the malignant transformation of HNSCC, genome-wide analysis including non-coding RNA molecules will be indispensable.

5. Conclusions

PXN was discovered by searching for oncogenic target genes of *miR-199-5p* and *miR-199-3p*, tumor suppressive miRNAs in HNSCC. Aberrant expression of *PXN* facilitated cancer cell migration and invasion, and its expression was closely associated with HNSCC molecular pathogenesis. Searching for target genes of tumor-suppressive miRNAs is an attractive strategy for exploring the molecular mechanism of HNSCC.

Supplementary Materials: The following are available online at <https://www.mdpi.com/article/10.3390/genes12121910/s1>. Figure S1: Chromosomal locations and mature sequences of the *miR-199* family. Figure S2: The expression levels of *miR-199* family. Figure S3: Functional assays following ectopic expression of *miR-199-5p* and *miR-199-3p*, Figure S4: Photomicrographs of cells subjected to invasion assays. Figure S5: Photomicrographs of cells subjected to wound healing assays. Figure S6: Correlations between *miR-199* family and putative target genes. Figure S7: Full-size images of the Western blots shown in Figure 5. Figure S8: Efficiency of siRNA-mediated *PXN* knockdown in HNSCC cell lines (SAS and Sa3 cells). Figure S9: Photomicrographs of cells subjected to invasion assays. Figure S10: Photomicrographs of cells subjected to wound healing assays. Table S1: Features of HNSCC cell lines. Table S2: Reagents used in this study. Table S3: Clinical features of three HNSCC cases used for immunohistochemical staining.

Author Contributions: Data curation, N.T., C.M., T.K. and N.K.; formal analysis, N.T., C.M. and S.A.; investigation, N.T., C.M., S.O., A.K. (Ayaka Koma), T.K. and N.K.; project administration, N.S.; supervision, T.H. and K.U.; writing—original draft, N.T. and N.S.; writing—review & editing, A.K. (Atsushi Kasamatsu). All authors have read and agreed to the published version of the manuscript.

Funding: This study was supported by JSPS KAKENHI grant numbers 19H03847, 19K09863, 19K18759, 20H03883, and 21K09577.

Institutional Review Board Statement: The study was conducted according to the Declaration of Helsinki, and approved by the Bioethics Committee of Chiba University (approval number: 28–65, 10 February 2015).

Informed Consent Statement: Informed consent was obtained from all subjects involved in the study.

Data Availability Statement: The results shown here are, in part, based upon data generated by the TCGA Research Network: <https://www.cancer.gov/tcga> (accessed on 10 April 2020). The data presented in this study are available on request from the corresponding author.

Conflicts of Interest: The authors declare no conflict of interest.

References

1. Bray, F.; Ferlay, J.; Soerjomataram, I.; Siegel, R.L.; Torre, L.A.; Jemal, A. Global cancer statistics 2018: GLOBOCAN estimates of incidence and mortality worldwide for 36 cancers in 185 countries. *CA Cancer J. Clin.* **2018**, *68*, 394–424. [[CrossRef](#)] [[PubMed](#)]
2. Johnson, D.E.; Burtneess, B.; Leemans, C.R.; Lui, V.W.Y.; Bauman, J.E.; Grandis, J.R. Head and neck squamous cell carcinoma. *Nat. Rev. Dis. Primers* **2020**, *6*, 92. [[CrossRef](#)]
3. Cramer, J.D.; Burtneess, B.; Le, Q.T.; Ferris, R.L. The changing therapeutic landscape of head and neck cancer. *Nat. Rev. Clin. Oncol.* **2019**, *16*, 669–683. [[CrossRef](#)]
4. Mehanna, H.; Paleri, V.; West, C.M.; Nutting, C. Head and neck cancer—Part 1: Epidemiology, presentation, and preservation. *Clin. Otolaryngol.* **2011**, *36*, 65–68. [[CrossRef](#)] [[PubMed](#)]
5. Sha, J.; Bai, Y.; Ngo, H.X.; Okui, T.; Kanno, T. Overview of Evidence-Based Chemotherapy for Oral Cancer: Focus on Drug Resistance Related to the Epithelial-Mesenchymal Transition. *Biomolecules* **2021**, *11*, 893. [[CrossRef](#)]
6. Chow, L.Q.M. Head and Neck Cancer. *N. Engl. J. Med.* **2020**, *382*, 60–72. [[CrossRef](#)] [[PubMed](#)]
7. Leemans, C.R.; Braakhuis, B.J.; Brakenhoff, R.H. The molecular biology of head and neck cancer. *Nat. Rev. Cancer* **2011**, *11*, 9–22. [[CrossRef](#)]
8. Cohen, E.E.W.; Soulières, D.; Le Tourneau, C.; Dinis, J.; Licitra, L.; Ahn, M.J.; Soria, A.; Machiels, J.P.; Mach, N.; Mehra, R.; et al. Pembrolizumab versus methotrexate, docetaxel, or cetuximab for recurrent or metastatic head-and-neck squamous cell carcinoma (KEYNOTE-040): A randomised, open-label, phase 3 study. *Lancet* **2019**, *393*, 156–167. [[CrossRef](#)]
9. Betel, D.; Wilson, M.; Gabow, A.; Marks, D.S.; Sander, C. The microRNA.org resource: Targets and expression. *Nucleic Acids Res.* **2008**, *36*, D149–D153. [[CrossRef](#)]
10. Anfossi, S.; Babayan, A.; Pantel, K.; Calin, G.A. Clinical utility of circulating non-coding RNAs—An update. *Nat. Rev. Clin. Oncol.* **2018**, *15*, 541–563. [[CrossRef](#)]
11. Nelson, K.M.; Weiss, G.J. MicroRNAs and cancer: Past, present, and potential future. *Mol. Cancer Ther.* **2008**, *7*, 3655–3660. [[CrossRef](#)] [[PubMed](#)]
12. Krek, A.; Grun, D.; Poy, M.N.; Wolf, R.; Rosenberg, L.; Epstein, E.J.; MacMenamin, P.; da Piedade, I.; Gunsalus, K.C.; Stoffel, M.; et al. Combinatorial microRNA target predictions. *Nat. Genet.* **2005**, *37*, 495–500. [[CrossRef](#)]
13. Rupaimoole, R.; Slack, F.J. MicroRNA therapeutics: Towards a new era for the management of cancer and other diseases. *Nat. Rev. Drug Discov* **2017**, *16*, 203–222. [[CrossRef](#)] [[PubMed](#)]
14. Tay, Y.; Rinn, J.; Pandolfi, P.P. The multilayered complexity of ceRNA crosstalk and competition. *Nature* **2014**, *505*, 344–352. [[CrossRef](#)]
15. Koshizuka, K.; Hanazawa, T.; Arai, T.; Okato, A.; Kikkawa, N.; Seki, N. Involvement of aberrantly expressed microRNAs in the pathogenesis of head and neck squamous cell carcinoma. *Cancer Metastasis Rev.* **2017**, *36*, 525–545. [[CrossRef](#)]
16. Koshizuka, K.; Hanazawa, T.; Kikkawa, N.; Arai, T.; Okato, A.; Kurozumi, A.; Kato, M.; Katada, K.; Okamoto, Y.; Seki, N. Regulation of ITGA3 by the anti-tumor miR-199 family inhibits cancer cell migration and invasion in head and neck cancer. *Cancer Sci.* **2017**, *108*, 1681–1692. [[CrossRef](#)]
17. Koma, A.; Asai, S.; Minemura, C.; Oshima, S.; Kinoshita, T.; Kikkawa, N.; Koshizuka, K.; Moriya, S.; Kasamatsu, A.; Hanazawa, T.; et al. Impact of Oncogenic Targets by Tumor-Suppressive miR-139-5p and miR-139-3p Regulation in Head and Neck Squamous Cell Carcinoma. *Int. J. Mol. Sci.* **2021**, *22*, 9947. [[CrossRef](#)]
18. Kozomara, A.; Birgaoanu, M.; Griffiths-Jones, S. miRBase: From microRNA sequences to function. *Nucleic Acids Res.* **2019**, *47*, D155–D162. [[CrossRef](#)]
19. Agarwal, V.; Bell, G.W.; Nam, J.W.; Bartel, D.P. Predicting effective microRNA target sites in mammalian mRNAs. *eLife* **2015**, *4*. [[CrossRef](#)] [[PubMed](#)]
20. Anaya, J. Linking TCGA survival data to mRNAs, miRNAs, and lncRNAs. *Peer J. Comput. Sci.* **2016**, *2*, e67. [[CrossRef](#)]
21. Subramanian, A.; Tamayo, P.; Mootha, V.K.; Mukherjee, S.; Ebert, B.L.; Gillette, M.A.; Paulovich, A.; Pomeroy, S.L.; Golub, T.R.; Lander, E.S.; et al. Gene set enrichment analysis: A knowledge-based approach for interpreting genome-wide expression profiles. *Proc. Natl. Acad. Sci. USA* **2005**, *102*, 15545–15550. [[CrossRef](#)]
22. Mootha, V.K.; Lindgren, C.M.; Eriksson, K.F.; Subramanian, A.; Sihag, S.; Lehar, J.; Puigserver, P.; Carlsson, E.; Ridderstråle, M.; Laurila, E.; et al. PGC-1alpha-responsive genes involved in oxidative phosphorylation are coordinately downregulated in human diabetes. *Nat. Genet.* **2003**, *34*, 267–273. [[CrossRef](#)] [[PubMed](#)]
23. Liberzon, A.; Subramanian, A.; Pinchback, R.; Thorvaldsdóttir, H.; Tamayo, P.; Mesirov, J.P. Molecular signatures database (MSigDB) 3.0. *Bioinformatics* **2011**, *27*, 1739–1740. [[CrossRef](#)] [[PubMed](#)]
24. Oshima, S.; Asai, S.; Seki, N.; Minemura, C.; Kinoshita, T.; Goto, Y.; Kikkawa, N.; Moriya, S.; Kasamatsu, A.; Hanazawa, T.; et al. Identification of Tumor Suppressive Genes Regulated by miR-31-5p and miR-31-3p in Head and Neck Squamous Cell Carcinoma. *Int. J. Mol. Sci.* **2021**, *22*, 6199. [[CrossRef](#)]
25. Hong, M.; Tao, S.; Zhang, L.; Diao, L.T.; Huang, X.; Huang, S.; Xie, S.J.; Xiao, Z.D.; Zhang, H. RNA sequencing: New technologies and applications in cancer research. *J. Hematol. Oncol.* **2020**, *13*, 166. [[CrossRef](#)] [[PubMed](#)]
26. Yamada, Y.; Koshizuka, K.; Hanazawa, T.; Kikkawa, N.; Okato, A.; Idichi, T.; Arai, T.; Sugawara, S.; Katada, K.; Okamoto, Y.; et al. Passenger strand of miR-145-3p acts as a tumor-suppressor by targeting MYO1B in head and neck squamous cell carcinoma. *Int. J. Oncol.* **2018**, *52*, 166–178. [[CrossRef](#)] [[PubMed](#)]

27. Okada, R.; Koshizuka, K.; Yamada, Y.; Moriya, S.; Kikkawa, N.; Kinoshita, T.; Hanazawa, T.; Seki, N. Regulation of Oncogenic Targets by miR-99a-3p (Passenger Strand of miR-99a-Duplex) in Head and Neck Squamous Cell Carcinoma. *Cells* **2019**, *8*, 1535. [[CrossRef](#)] [[PubMed](#)]
28. Mitra, R.; Adams, C.M.; Jiang, W.; Greenawalt, E.; Eischen, C.M. Pan-cancer analysis reveals cooperativity of both strands of microRNA that regulate tumorigenesis and patient survival. *Nat. Commun.* **2020**, *11*, 968. [[CrossRef](#)] [[PubMed](#)]
29. Wang, Q.; Ye, B.; Wang, P.; Yao, F.; Zhang, C.; Yu, G. Overview of microRNA-199a Regulation in Cancer. *Cancer Manag. Res.* **2019**, *11*, 10327–10335. [[CrossRef](#)]
30. Wei, D.; Wang, W.; Shen, B.; Zhou, Y.; Yang, X.; Lu, G.; Yang, J.; Shao, Y. MicroRNA-199a-5p suppresses migration and invasion in oral squamous cell carcinoma through inhibiting the EMT-related transcription factor SOX4. *Int. J. Mol. Med.* **2019**, *44*, 185–195. [[CrossRef](#)]
31. Wei, D.; Shen, B.; Wang, W.; Zhou, Y.; Yang, X.; Lu, G.; Yang, J.; Shao, Y. MicroRNA-199a-5p functions as a tumor suppressor in oral squamous cell carcinoma via targeting the IKK β /NF- κ B signaling pathway. *Int. J. Mol. Med.* **2019**, *43*, 1585–1596. [[CrossRef](#)]
32. Jin, X.; Zhai, B.; Fang, T.; Guo, X.; Xu, L. FXR1 is elevated in colorectal cancer and acts as an oncogene. *Tumour Biol.* **2016**, *37*, 2683–2690. [[CrossRef](#)]
33. Qian, J.; Chen, H.; Ji, X.; Eisenberg, R.; Chakravarthy, A.B.; Mayer, I.A.; Massion, P.P. A 3q gene signature associated with triple negative breast cancer organ specific metastasis and response to neoadjuvant chemotherapy. *Sci. Rep.* **2017**, *7*, 45828. [[CrossRef](#)] [[PubMed](#)]
34. Comtesse, N.; Keller, A.; Diesinger, I.; Bauer, C.; Kayser, K.; Huwer, H.; Lenhof, H.P.; Meese, E. Frequent overexpression of the genes FXR1, CLAPM1 and EIF4G located on amplicon 3q26-27 in squamous cell carcinoma of the lung. *Int. J. Cancer* **2007**, *120*, 2538–2544. [[CrossRef](#)]
35. Qie, S.; Majumder, M.; Mackiewicz, K.; Howley, B.V.; Peterson, Y.K.; Howe, P.H.; Palanisamy, V.; Diehl, J.A. Fbxo4-mediated degradation of Fxr1 suppresses tumorigenesis in head and neck squamous cell carcinoma. *Nat. Commun.* **2017**, *8*, 1534. [[CrossRef](#)] [[PubMed](#)]
36. Majumder, M.; House, R.; Palanisamy, N.; Qie, S.; Day, T.A.; Neskey, D.; Diehl, J.A.; Palanisamy, V. RNA-Binding Protein FXR1 Regulates p21 and TERC RNA to Bypass p53-Mediated Cellular Senescence in OSCC. *PLoS Genet.* **2016**, *12*, e1006306. [[CrossRef](#)]
37. Majumder, M.; Palanisamy, V. RNA binding protein FXR1-miR301a-3p axis contributes to p21WAF1 degradation in oral cancer. *PLoS Genet.* **2020**, *16*, e1008580. [[CrossRef](#)]
38. Brown, M.C.; Turner, C.E. Paxillin: Adapting to change. *Physiol. Rev.* **2004**, *84*, 1315–1339. [[CrossRef](#)] [[PubMed](#)]
39. Mitra, S.K.; Hanson, D.A.; Schlaepfer, D.D. Focal adhesion kinase: In command and control of cell motility. *Nat. Rev. Mol. Cell Biol.* **2005**, *6*, 56–68. [[CrossRef](#)]
40. Wozniak, M.A.; Modzelewska, K.; Kwong, L.; Keely, P.J. Focal adhesion regulation of cell behavior. *Biochim. Biophys. Acta* **2004**, *1692*, 103–119. [[CrossRef](#)]
41. Zhou, J.; Yi, Q.; Tang, L. The roles of nuclear focal adhesion kinase (FAK) on Cancer: A focused review. *J. Exp. Clin. Cancer Res.* **2019**, *38*, 250. [[CrossRef](#)]
42. Chen, Y.; Zhao, H.; Xiao, Y.; Shen, P.; Tan, L.; Zhang, S.; Liu, Q.; Gao, Z.; Zhao, J.; Zhao, Y.; et al. Pan-cancer analysis reveals an immunological role and prognostic potential of PXN in human cancer. *Aging* **2021**, *13*, 16248–16266. [[CrossRef](#)] [[PubMed](#)]
43. Deakin, N.O.; Pignatelli, J.; Turner, C.E. Diverse roles for the paxillin family of proteins in cancer. *Genes Cancer* **2012**, *3*, 362–370. [[CrossRef](#)] [[PubMed](#)]
44. Jiang, H.; Zhang, H.; Hu, X.; Li, W. Knockdown of long non-coding RNA XIST inhibits cell viability and invasion by regulating miR-137/PXN axis in non-small cell lung cancer. *Int. J. Biol. Macromol.* **2018**, *111*, 623–631. [[CrossRef](#)] [[PubMed](#)]
45. Yan, J.; Jia, Y.; Chen, H.; Chen, W.; Zhou, X. Long non-coding RNA PXN-AS1 suppresses pancreatic cancer progression by acting as a competing endogenous RNA of miR-3064 to upregulate PIP4K2B expression. *J. Exp. Clin. Cancer Res.* **2019**, *38*, 390. [[CrossRef](#)] [[PubMed](#)]
46. Yuan, J.H.; Liu, X.N.; Wang, T.T.; Pan, W.; Tao, Q.F.; Zhou, W.P.; Wang, F.; Sun, S.H. The MBNL3 splicing factor promotes hepatocellular carcinoma by increasing PXN expression through the alternative splicing of lncRNA-PXN-AS1. *Nat. Cell Biol.* **2017**, *19*, 820–832. [[CrossRef](#)] [[PubMed](#)]
47. Xu, J.; Zhang, P.; Sun, H.; Liu, Y. LINC01094/miR-577 axis regulates the progression of ovarian cancer. *J. Ovarian Res.* **2020**, *13*, 122. [[CrossRef](#)] [[PubMed](#)]
48. Xiao, Z.S.; Long, H.; Zhao, L.; Li, H.X.; Zhang, X.N. LncRNA HOTTIP promotes proliferation and inhibits apoptosis of gastric carcinoma cells via adsorbing miR-615-3p. *Eur. Rev. Med. Pharmacol. Sci.* **2020**, *24*, 6692–6698. [[CrossRef](#)] [[PubMed](#)]
49. Cui, Y.; Zhang, C.; Lian, H.; Xie, L.; Xue, J.; Yin, N.; Guan, F. LncRNA linc00460 sponges miR-1224-5p to promote esophageal cancer metastatic potential and epithelial-mesenchymal transition. *Pathol. Res. Pract.* **2020**, *216*, 153026. [[CrossRef](#)] [[PubMed](#)]
50. Chen, A.Y.; Zhang, K.; Liu, G.Q. LncRNA LINP1 promotes malignant progression of pancreatic cancer by adsorbing microRNA-491-3p. *Eur. Rev. Med. Pharmacol. Sci.* **2020**, *24*, 9315–9324. [[CrossRef](#)]
51. Li, P.; Wang, L.; Li, P.; Hu, F.; Cao, Y.; Tang, D.; Ye, G.; Li, H.; Wang, D. Silencing lncRNA XIST exhibits antiproliferative and proapoptotic effects on gastric cancer cells by up-regulating microRNA-132 and down-regulating PXN. *Aging* **2020**, *13*, 14469–14481. [[CrossRef](#)] [[PubMed](#)]

52. Du, C.; Wang, Y.; Zhang, Y.; Zhang, J.; Zhang, L.; Li, J. LncRNA DLX6-AS1 Contributes to Epithelial-Mesenchymal Transition and Cisplatin Resistance in Triple-negative Breast Cancer via Modulating Mir-199b-5p/Paxillin Axis. *Cell Transplant.* **2020**, *29*, 963689720929983. [[CrossRef](#)]
53. Liu, Z.; Mao, L.; Wang, L.; Zhang, H.; Hu, X. miR-218 functions as a tumor suppressor gene in cervical cancer. *Mol. Med. Rep.* **2020**, *21*, 209–219. [[CrossRef](#)] [[PubMed](#)]
54. Li, X.; He, J.; Shao, M.; Cui, B.; Peng, F.; Li, J.; Ran, Y.; Jin, D.; Kong, J.; Chang, J.; et al. Downregulation of miR-218-5p promotes invasion of oral squamous cell carcinoma cells via activation of CD44-ROCK signaling. *Biomed. Pharmacother.* **2018**, *106*, 646–654. [[CrossRef](#)] [[PubMed](#)]
55. Wu, D.W.; Chuang, C.Y.; Lin, W.L.; Sung, W.W.; Cheng, Y.W.; Lee, H. Paxillin promotes tumor progression and predicts survival and relapse in oral cavity squamous cell carcinoma by microRNA-218 targeting. *Carcinogenesis* **2014**, *35*, 1823–1829. [[CrossRef](#)] [[PubMed](#)]
56. Kinoshita, T.; Hanazawa, T.; Nohata, N.; Kikkawa, N.; Enokida, H.; Yoshino, H.; Yamasaki, T.; Hidaka, H.; Nakagawa, M.; Okamoto, Y.; et al. Tumor suppressive microRNA-218 inhibits cancer cell migration and invasion through targeting laminin-332 in head and neck squamous cell carcinoma. *Oncotarget* **2012**, *3*, 1386–1400. [[CrossRef](#)]